Facile Synthesis of Mesoporous Gold−Silica Nanocomposite Materials via Sol−Gel Process with Nonsurfactant Templates

Shan Cheng,[†] Yen Wei,*[,†] Qiuwei Feng,[†] Kun-Yuan Qiu,[‡] Jie-Bin Pang,[‡] Susan A. Jansen,[§] Ray Yin,[||] and Kate Ong[†,||]

Department of Chemistry, Drexel University, Philadelphia, Pennsylvania 19104, Department of Polymer Science & Engineering, Peking University, Beijing 100871, China, Department of Chemistry, Temple University, Philadelphia, Pennsylvania 19122, and US Army Research Laboratory, Aberdeen Proving Ground, Maryland 21005

Received February 13, 2002. Revised Manuscript Received November 6, 2002

Mesoporous gold−silica nanocomposites have been synthesized through simple one-step sol−gel reactions of tetraethyl orthosilicate (TEOS) with a gold sol in the presence of dibenzoyl tartaric acid (DBTA) as a nonsurfactant template. The gold nanoparticles were incorporated into the three-dimensional silica network through the sol−gel process to afford monolithic crack-free DBTA-containing gold−silica gels. After removal of DBTA by calcination at 550 °C, annealed mesoporous gold−silica nanocomposites were obtained. The pore structure parameters were investigated by means of nitrogen sorption isotherm, X-ray diffraction, and transmission electron microscopy (TEM). The results indicate that the mesoporous structure of the gold−silica nanocomposites has high surface areas up to 630 m^2/g, large pore volume of ∼0.5 cm^3/g, and pore diameters of 3−4 nm with relatively narrow pore size distributions. With use of energy-dispersive X-ray (EDX) elemental analysis, the compositions of the gold−silica composite materials were quantitatively measured. The effects of gold content on the pore parameters have been addressed. The TEM and X-ray mapping images show that gold particles in the range of 2−8 nm are homogeneously distributed throughout the silica matrixes for all the samples. The surface plasmon resonance of gold nanoparticles was also investigated.

Introduction

Nanoscale dispersions of metal and semiconductor in silicate and other metal oxide matrixes have attracted great interest because of their unique size-dependent optical, electrical, and chemical properties.[1−6] Not only interesting from a scientific point of view, these sol−gel-derived composite materials also exhibit distinctive advantages for practical sensing[7,8] and catalysis applications[9−11] because of the following: (1) the high porosity of a sol−gel matrix (silica, titania, and zirconia) allows for a fast mass exchange between active sites and surroundings; (2) the optical properties of the nanocrystalline dispersant are only slightly affected by the transparent matrix; and (3) materials may be readily cast in a variety of forms (monolith, thin film, coating, etc.).[12, 13]

Several general strategies were reported for the encapsulation of metallic colloids in sol−gel matrixes. With use of an inverse micelle technique, spherical nanosized metal−silica composite particles were prepared via a sol−gel reaction within the metal alkoxide microemulsion.[14] Martino et al. reported the synthesis of metal nanocluster-dispersed silica monoliths by diffusing the metal clusters into pre-existing wet monoliths formed through a sol−gel reaction.[15] Silica thin films and bulk materials containing metal colloids were also prepared by diffusing metal salt solution into silica matrixes, followed by a reduction of the metal salt, which could be chemical, photochemical, or sonochemi-

* To whom correspondence should be addressed.
[†] Drexel University.
[‡] Peking University.
[§] Temple University.
[||] US Army Research Laboratory.

(1) (a) Bharathi, S.; Nogami, M.; Lev, O. *Langmuir* **2001**, *17*, 2602. (b) Nogami, M. *Ceram. Trans.* **1998**, *81*, 255.
(2) Epifani, M.; Carlino, E.; Blasi, C.; Giannini, C.; Tapfer, L.; Vasanelli, L. *Chem. Mater.* **2001**, *13*, 1533.
(3) Bronstein, L. M.; Polarz, S.; Smarsly, B.; Antonietti, M. *Adv. Mater.* **2001**, *13*, 1333.
(4) Khushalani, D.; Hasenzahl, S.; Mann, S. *J. Nanosci. Nanotechnol.* **2001**, *1*, 129.
(5) Hayakawa, T.; Ono, Y.; Nogami, M. *Proc. SPIE-Int. Soc. Opt. Eng.* **2000**, *3943*, 102.
(6) Anderson, M. L.; Morris, C. A.; Stroud, R. M.; Merzbacher, C. I.; Rolison, D. R. *Langmuir* **1999**, *15*, 674.
(7) Bharathi, S.; Nogami, M. *Analyst* **2001**, *126*, 1919.
(8) Lee, Y.-H.; Farquharson, S.; Kwon, H.; Shahriari, M.; Rainey, P. *SPIE-Int. Soc. Opt. Eng.* **1999**, *3537*, 252.
(9) Claus, P.; Brueckner, A.; Mohr, C.; Hofmeister, H. *J. Am. Chem. Soc.* **2000**, *122*, 11430.
(10) Rath, A.; Aceves, E.; Mitome, J.; Liu, J.; Ozkan, U. S.; Shore, S. G. J. *Mol. Catal. A: Chem.* **2001**, *165*, 103.
(11) Valden, M.; Lai, X.; Goodman, D. W. *Science* **1998**, *11*, 1647.
(12) De, G. *J. Sol-Gel Sci. Technol.* **1998**, *1*, 289.
(13) (a) Scott, B. J.; Wirnsberger, G.; Stucky, G. D. *Chem. Mater.* **2001**, *13*, 3140. (b) Innocenzi, P.; Brusatin, G.; Martucci, A.; Urabe, K. *Thin Solid Films* **1996**, *279*, 23.
(14) Li, T.; Moon, J.; Morrone, A. A.; Mecholsky, J. J.; Talham, D. R.; Adair, J. H. *Langmuir* **1999**, *15*, 4328.
(15) Martino, A.; Yamamaka, S. A.; Kawola, J. S.; Loy, D. L. *Chem. Mater.* **1997**, *9*, 423.

10.1021/cm0202106 CCC: $25.00
Published on Web 03/12/2003

cal reduction.[16,17] Using a two-step sol−gel procedure, Whilton et al.[18] synthesized porous silica-supported metal nanoparticles. Prefabricated metal−polymer microgel hybrids were incorporated in a silica matrix. In this method, the spherical functionalized polymer microgels function as both nanosized exotemplates for controlled growth of metal colloids and as endotemplates for porous sol−gel silica. From all these works, it has been noticed that the morphology and properties of the metal−silica composite were greatly affected by the preparation methods.

We have been interested in the nanoscale dispersions of noble metal (Au or Ag) particles in mesoporous sol−gel materials. With a size range of 2−50 nm, the mesopores permit ingress by molecules and guests physically excluded from microporous materials and provide a high surface area available for sensing and catalysis. In comparison to macroporous materials, the pore size can be made small enough to prevent the active species (i.e., nanosized particles) from leaking out of the matrixes. Since the early 1990s, numerous kinds of mesoporous silicate have been prepared using neutral or ionic surfactant as the template or pore-forming agent.[19,20] Recently, our group developed a novel, low-cost, biocompatible nonsurfactant pathway for preparing mesoporous materials.[21] With use of small nonsurfactant molecules such as glucose, fructose, dibenzoyl tartaric acid (DBTA), and urea as a pore forming-agent, silica mesoporous materials have been prepared with high surface area (∼1000 m^2/g) and pore volume (∼0.5−1.0 cm^3/g). The pore size is in the range of 2−6 nm with narrow distributions.[22,23]

In this work, we have successfully applied this convenient nonsurfactant-templating approach to the synthesis of mesoporous gold−silica nanocomposites. Instead of using a postdiffusion process, monolithic gold−silica nanocomposites were synthesized through a one-step sol−gel reaction in the presence of a colloidal gold sol and a nonsurfactant template in the starting precursor sol mixtures. After the template was removed through calcinations, the materials exhibited mesoporosity with a high surface area up to 600 m^2/g, a pore volume of ∼0.5 cm^3/g, and relatively narrow pore size distributions with a pore diameter of 3−4 nm. Gold particles ranging in diameters of 2−8 nm were homogeneously dispersed throughout the silica matrix. The gold−silica composites are nanoscopic materials in which the optical and physical/chemical properties of gold nanoparticles are coupled with the high surface area and the high porosity of the silica framework.

Experimental Section

Materials and Synthesis. Tetraethyl orthosilicate (TEOS, Aldrich), tetrahydrofuran (THF, Aldrich), dibenzoyl tartaric acid (DBTA, Aldrich), hydrochloric acid (HCl, Fisher), and Liquid Bright Gold 5154 (Engelhard Corporation) were all used as received without further purification.

Mesoporous gold−silica nanocomposites were synthesized through a simple one-step sol−gel process in the presence of DBTA as a nonsurfactant template. With a stabilizing agent, Liquid Bright Gold 5154 is a colloidal gold solution, which contains 5 wt % metallo-organic gold compound in cyclohexanone. It is widely used for gold coating on glass and ceramics with good adhesion properties. To prepare the composite, the colloidal gold sol was combined with a prehydrolyzed silica sol and the template solution. As the sol mixture gelled, the gold sol was incorporated into the three-dimensional silica network. After being aged and dried at room temperature, the resulting material was subjected to calcination to remove the template and anneal the gold−silica composite. With the DBTA template concentration of 50 wt %, which is calculated based on the weight of silicon dioxide and the template in the final dry product (excluding gold content), a series of samples with different gold contents were prepared. In this work the DBTA template content was fixed at 50 wt % since the effect of nonsurfactant template on pore structure of silica matrix has been established and previously reported.[21,22] The amount of gold sol used was varied from 10 to 25 wt %, based on the weight of TEOS employed. The exact gold content of the final composite materials was determined by elemental analysis with energy-dispersive X-ray (EDX). As a typical procedure for preparing the sample GS50-10 containing 10 wt % gold sol, 4.16 g of TEOS (0.02 mol), 8.79 g of THF (0.12 mol), 1.44 g of H_2O (0.08 mol), and 0.100 mL of 2 M HCl (0.20 mmol) were mixed in a 50-mL beaker and magnetically stirred at room temperature for 4 h. The template solution was prepared by dissolving 1.20 g of DBTA (50 wt % based on the weight of silica dioxide and the template in the final dry product) in 1.00 g of THF and then was added into the hydrolyzed TEOS sol. After 30 min under gentle stirring, 0.42 g of Liquid Bright Gold 5154 (10 wt % based on TEOS) was added. The resulting dark brown mixture was homogeneous and slightly translucent. The beaker was then covered with a piece of paraffin film. After 1−2 h, the beaker was removed from the stirring plate. Approximately 15−20 pinholes were punched on the paraffin film to allow the evaporation of the solvent and volatile byproducts of the sol−gel reactions, for example, ethanol and water. The sol−gel reaction proceeded at room temperature for about 8 days. On drying, dark-brown opaque and monolithic DBTA-containing gold−silica gel was obtained. The sample was further dried under vacuum for 10 days, during which it broke into smaller, but crack-free, pieces. Two control samples were prepared in the absence of either gold sol or DBTA template under otherwise identical conditions.

To obtain mesoporous gold−silica nanocomposites, the as-synthesized samples were ground into a fine powder and subjected to calcination in air for a period of 16 h at 550 °C, with a heating rate of 0.5 °C/min. After the calcination, the sample turned a wine-red color because of the surface plasmon resonance of gold nanoparticles.

Instrumentation and Characterization. The N_2 sorption characterization was conducted on a Micromeritics ASAP 2010 surface area and pore size analyzer (Micromeritics Inc., Norcross, GA) at −196 °C. All samples were degassed at 200 °C and 1 Pa for at least 6 h prior to N_2 adsorption−desorption isotherm measurement. Powder XRD patterns were recorded on a Siemens D500 diffractometer equipped with a rotating anode and using Cu Kα radiation (λ = 0.15418 nm). EDX elemental analysis and X-ray mapping were conducted on an EDX interfaced AMRAY 1830 scanning electron microscope

(16) Sakka, S.; Kozuka, H. *J. Sol-Gel Sci. Technol.* **1998**, *13*, 701.
(17) Chen, W.; Cai, W. P.; Liang, C. H.; Zhang, L. D. *Mater. Res. Bull.* **2001**, *36*, 335.
(18) Whilton, N. T.; Berton, B.; Bronstein, L.; Hentze, H. P.; Antonietti, M. *Adv. Mater.* **1999**, *11*, 1014.
(19) Kresge, C. T.; Leonowicz, M. E.; Roth, W. J.; Vartuli, J. C.; Beck, J. S. *Nature* **1992**, *359*, 710.
(20) For recent reviews, see: (a) Schueth, F.; Schmidt, W. *Adv. Eng. Mater.* **2002**, *4*, 269. (b) Soten, I.; Ozin, G. A. *Supramolecular Organization and Materials Design*; Jones, W., Rao, C. N. R., Eds.; Cambridge University Press: Cambridge, UK, 2002; p 34. (c) Stein, A.; Melde, B. J. *Surf. Sci. Ser.* **2001**, *100*, 819. (d) Ciesla, U.; Schuth, F. *Microporous Mesoporous Mater.* **1999**, *27*, 131. (e) Ying, J. Y.; Mehnert, C. P.; Wong, M. S. *Angew. Chem., Int. Ed.* **1999**, *38*, 56.
(21) Wei, Y.; Jin, D.; Ding, T.; Shih, W.-H.; Liu, X.; Cheng, S. Z. D.; Fu, Q. *Adv. Mater.* **1998**, *10*, 313.
(22) Wei, Y.; Xu, J.; Dong, H.; Dong, J.; Qiu, K.; Jansen-Varnum, S. A. *Chem. Mater.* **1999**, *11*, 2023.
(23) (a) Pang, J. B.; Qiu, K. Y.; Wei, Y.; Lei, X.; Liu, Z. F. *Chem. Commun.* **2000**, *6*, 477. (b) Pang, J. B.; Qiu, K. Y.; Wei, Y. *Chem. Mater.* **2001**, *14*, 2361. (c) Wei, Y.; Dong, H.; Feng, Q. *ChemPhysChem*. **2002**, *3* (9), 803.

Table 1. Compositions and Pore Parameters of the Gold−Silica Composite Samples Prepared in the Presence of 50 wt % DBTA Template (i.e., GS50- Samples) or without DBTA Template (i.e., GS0-50 Sample).

sample code[a]	gold[b] (wt %) before extraction	gold[b] (wt %) after extraction	S_{BET} (m^2/g)	V_{PORE} (cm^3/g)	D_{BJH} (nm)	micropore volume[c] (cm^3/g)
GS50-0	0.0	0.0	596	0.48	3.6	0.08
GS50-10	6.9	5.9	629	0.42	3.0	0.07
GS50-20	10.1	7.8	573	0.39	3.1	0.09
GS50-25	11.4	11.4	212	0.17	3.5	0.03
GS0-50	17.4	15.8	108	0.13	4.2	

[a] The numerical figure in the sample code denotes the DBTA template concentration (wt % of silicon dioxide and template in the final dry product, excluding gold content) and gold sol content (wt % of TEOS) in the starting materials, respectively. [b] Average values calculated based on EDX elemental analysis taken at four different areas of each sample after the calcination. [c] Values determined from the t-plot analysis.

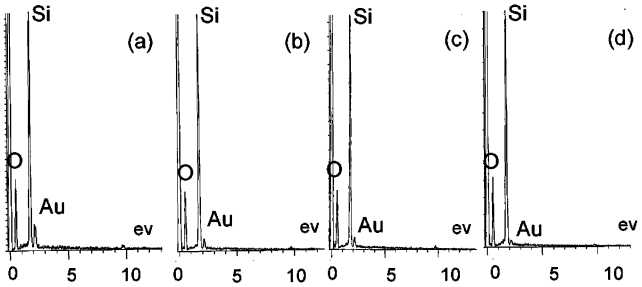

Figure 1. Representative X-ray energy-dispersive spectra for gold−silica nanocomposite: (a) GS0-50; (b) GS50-25; (c) GS50-20; (d) GS50-10.

(SEM). The instrument was operated at an accelerating voltage of 5 kV. The samples were deposited on sample holders with adhesive carbon tape. TEM images of the gold−silica nanocomposites were obtained with Hitachi H-9000 HRTEM operated at an accelerating voltage of 300 kV. The TEM samples were prepared by evaporation of pre-made ethyl alcohol suspensions of the finely grounded sample powder on a Cu grid coated with holey C film. Solid-state UV−visible reflectance spectra of the as-synthesized samples were measured with a Perkin-Elmer-330 spectrophotometer. The baseline of the instrument was calibrated with magnesium carbonate powder. The samples were prepared by spreading a layer of silica−gold nanocomposite fine powder on the top of a layer of magnesium carbonate in a quartz sample holder. All the spectra were obtained at a scanning rate of 180 nm/min.

Results and Discussions

In the presence of DBTA as a nonsurfactant template, mesoporous gold−silica nanocomposite materials were prepared using a sol−gel process, combining a gold sol and a prehydrolyzed silica sol. As nanosized gold phases dispersed in the three-dimensional mesoporous silica network, the composites were prepared with the various gold contents at a fixed DBTA template content of 50 wt %. The compositions and pore parameters of porous gold−silica composites are summarized in Table 1. The compositions were determined by elemental analysis with the EDX technique (Figure 1). The results show that in the final composite materials gold content is increased from 6.9 to 11.4 wt %, which is consistent with the trend of gold sol stoichiometry in the starting sol mixture. To examine the confining ability of the porous silica matrixes over the gold particles, the gold contents of the composites were investigated after extracting the mesoporous gold−silica samples with THF in a Soxhlet

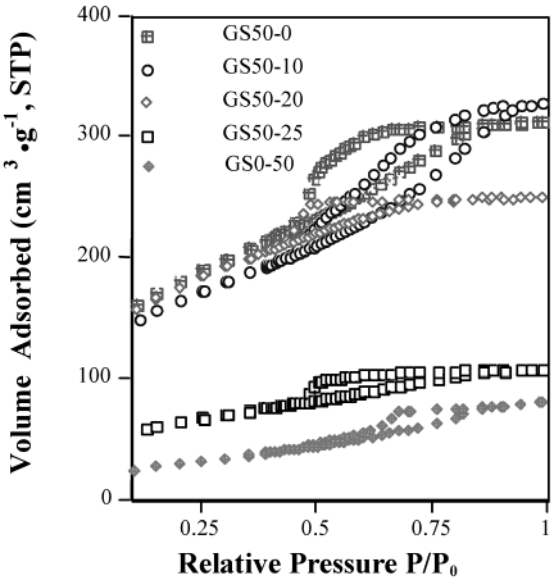

Figure 2. N_2 adsorption−desorption isotherms at −196 °C for the annealed gold−silica nanocomposite samples with varied gold content after removal of DBTA template.

apparatus for 5 h. The results are also summarized in Table 1. For all the gold-containing samples, after solvent extraction, more than 85% of the gold particles are not washed out and are still retained in the porous composite. This indicates a good confinement of active species (i.e., gold nanoparticles) in the mesoporous silica matrixes with low leakage.

Representative nitrogen adsorption−desorption isotherms at −196 °C for the porous gold−silica nanocomposite samples after the calcinations are shown in Figure 2. All the samples show type-IV-like isotherms with H2 hysteresis loops at P/P_0 of ∼0.4−0.8. The isotherm of the control sample in the absence of gold (i.e., SG50-0) containing 50 wt % DBTA is similar to that of typical nonsurfactant templated mesoporous silica materials, which we reported on earlier.[21] With the gold content at 10.1 wt % or lower, the pore structures of the composite samples are comparable to the control sample in the absence of gold. These materials exhibit mesoporosity with a pore diameter of 3−4 nm, a high Brunauer−Emmett−Teller (BET) surface area up to 630 m^2/g, and a large pore volume of ∼0.5 cm^3/g. On the basis of the t-plot analysis, the contributions from micropores to the pore volume are relatively small (Table 1). It should be noted that, with the gold content as low as 6.9 wt %, the composite sample (i.e., GS50-10) shows a higher BET surface area than the gold-free control sample (i.e., GS50-0). This phenomenon is not unexpected. During the sol−gel process, the organic moieties in the starting liquid gold sol might be trapped in the gold−silica matrix and may function as "co-templates" with DBTA. As the gold concentration is further increased, the BET surface area of the composite samples tends to decrease. When the gold content is increased to 11.4 wt %, the pore diameter remains at 3.5 nm. However, the surface area decreases to ∼210 m^2/g, and a smaller value of pore volume (∼0.17 cm^3/g) was observed. There could be several factors that might contribute to the observed decrease in the specific area and pore volume. First of all, more gold nanoparticles should result in smaller specific area and pore

volume because of the physical occupation of the internal space by the gold particles. However, such a space occupation cannot count for all the decreases.[24] There must be other factors. Indeed, as discussed later in this article, the gold particle size is slightly greater than the pore size, indicating that in some area the gold particles could have partially extruded into the pore walls made of relatively "soft" amorphous sol−gel silica. In such a case, the pore or channel in the silica matrix would be blocked and become inaccessible to the pore volume and surface area measurement. This should also contribute significantly to the observed low pore volume and specific area in the samples with high gold loadings. In addition, the presence of gold may also affect the interactions, for example, hydrogen bonding, between the nonsurfactant template (i.e., DBTA) and silicate species during the mesophase formation, which could result in modified pore parameters. Furthermore, it is possible that the introduction of gold into the silica matrix also brings complexities in porosity measurement with nitrogen sorptions, among which electrostatic forces between an adsorbate (i.e., nitrogen) and metallic surface and increased material density may affect the measured values to some extent.[25] Nevertheless, the nature and extent of such effects remain to be established qualitatively and quantitatively. Further investigation is in progress in our laboratories to access all these effects.

In all, with the introduction of gold sol, there simultaneously exist two factors affecting, in an opposite way, the porosity of the composite materials. One, as described above, results from co-templates, which increase the total pore surface area. The other factor is "the presence of gold" that reduces the surface area. The outcome depends on the compromise of these two factors: at low gold content, the pore surface area reduced by the gold coating is compensated, or even overcome, by the co-templating effect. As a result, the composite materials persist in a relatively high surface area and pore volume. While as the gold content increases, the co-template effect gradually becomes negligible, giving rise to decreased surface area. To confirm the co-templating effect, a control sample without DBTA, GS0-50, was prepared only with the gold sol (50 wt % of the weight of TEOS, corresponding to 17.4 wt % gold in composite) and a prehydrolyzed silica sol. The nitrogen sorption measurement shows that, despite shifting to a lower adsorbed volume, the isotherm of GS0-50 (Figure 2) still resembles a type-IV pattern with small H2 hysteresis loops at P/P_0 of ~0.7, which is indicative of certain porosity. Compared with the sample prepared only using DBTA as template (i.e., GS50-0), this control sample templated only by gold sol (i.e., GS0-50) shows a slightly larger pore diameter. This explains the trend that the pore diameter for all nanocomposites tend to increase as the gold sol concentration is increased, even though with the introduction of gold particles the pore diameter of the composites is over all smaller than the gold-free sample (GS50-0).

The Barrett−Joyner−Halenda (BJH) pore size distribution curves derived from desorption branches of the nitrogen isotherms are shown in Figure 3. With differential volumes plotted against pore diameter, the curves indicate relatively narrow pore size distributions with a peak pore diameter centered at 3−4 nm for all DBTA templated samples. The control sample prepared only with gold sol exhibits a much broader pore size distribution without a distinct, dominant pore size in the mesopore range (GS0-50 in Figure 3). The BJH pore size distributions derived from the adsorption branches are considerably broader, which are quite similar to those in the literature.[22] The pore size distribution derived from the desorption branch of a type-IV isotherm with a H2 hysteresis loop is usually believed to associate with the size distribution of the narrow neck of pores with an "ink bottle" shape. It is now more recognized that this may be oversimplified and that the role of network effect should be taken into the consideration when interpreting the pore shape and size derived from isotherm measurement.[26] Despite the complexity and the uncertainty in using the gas sorption measurement to determine the pore size and distribution, this method still provides us a good estimation of the pore structures of the porous materials. The pore diameters derived from the BJH method have been found to be in favorable agreement with those obtained from XRD and the TEM image analysis as discussed below.

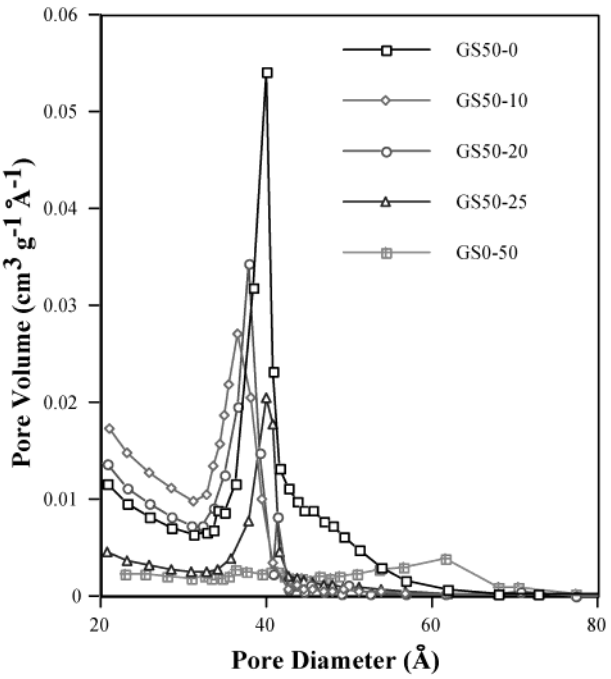

Figure 3. BJH pore size distribution curves of the mesoporous gold−silica nanocomposite derived from desorption isotherm branches.

All the mesoporous gold−silica samples exhibit a similar powder XRD profile, which is exemplified by sample GS50-10 in Figure 4. The XRD pattern shows an intense peak at a *d*-spacing of 6.3 nm along with a broad shoulder at low-angle range. A broad diffraction

(24) Suggested by a reviewer of this manuscript, gold particle occupation may not count for the surface area and pore volume decrease for high gold content samples. We appreciate the valuable comments by the reviewer on this discussion.

(25) Gregg, S. J.; Sing, K. S. W. *Adsorption, Surface Area and Porosity*, 2nd ed.; Academic Press: London, 1982.

(26) (a) Lee, C. K.; Chiang, A. S. T.; Tsay, C. S. *Key Eng. Mater.* **1995**, *115*, 21. (b) Sing, K. S. W.; Everett D. H.; Haul, R. A. W.; Moscou, L.; Pierotti, R. A.; Rouquèrol, J.; Siemieniewska, T. *Pure Appl. Chem.* **1995**, *57*, 603.

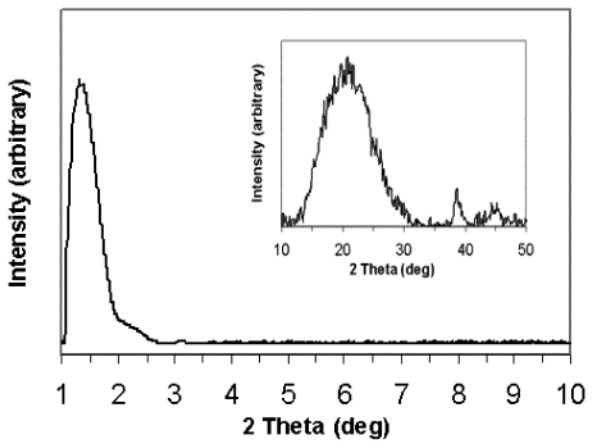

Figure 4. Powder XRD patterns for the mesoporous gold−silica nanocomposite sample GS50-10.

peak centered at 2θ of 21° was observed at high-angle range. This pattern is characteristic of a mesoporous structure lacking a long-range order, which is reminiscent of the disordered worm-hole-like mesoporous silicas prepared by a nonsurfactant templating pathway.[21−23,27] The analogous XRD patterns were also observed from some mesoporous materials obtained with neutral and cationic surfactant templates.[28−31,34] In the worm-hole-like porous structure, *d*-spacing obtained from XRD could be approximately the repeating distance from one layer of silica wall to the next layer of silica wall crossing a mesopore space. From the difference of the repeating distance (6.3 nm) and the average pore diameter (3.0 nm), the thickness of pore wall can be estimated to be ∼3.3 nm, which is comparable with those of the mesoporous materials prepared by a nonionic surfactant templating route[32,33] or cationic surfactant templated multiprecursors sol−gel method.[34] The presence of a single broad peak centered at a 2θ value of 21° is attributed to the amorphous structure of sol−gel silica.[21]

Besides the nitrogen sorption and XDR measurements, the porous structure of the silica matrixes and the morphology of the gold nanoparticles formed within the mesopores (or channels) of the materials were further studied using transmission electron microscopy (TEM). As shown in Figure 5a, nearly spherical gold particles with the size varying from 2 to 8 nm but centered at ∼4 nm in diameter were randomly scattered in the silica porous matrix. As one can see in Figure 3, the pore size is not strictly uniform and it does have a distribution. Such a pore size distribution generally reflects the observed gold particle size distribution (Figure 5b). The peak gold particle size (Figure 5b) is about 4 nm, which agrees reasonably well with, but is somewhat larger than, the BJH peak pore size of ca. 3.5 nm (GS50-10 in Figure 3). Some of the gold particles may intrude into the sol−gel silica walls, leading to a partial blockage of the mesopores and channels. The overall composite matrix exhibits a disordered, interconnected, worm-hole-like pore structure with an average pore diameter of 3−5 nm. The observed pore structure is similar to those of the mesoporous silica materials prepared with nonsurfactant templates reported in the literature.[21−23,27] As shown in the insert of Figure 5a, the electron diffraction of the gold nanoparticle shows a series of spots symmetrically distributed along concentric rings, which is indicative of a well-defined crystalline structure. On the basis of the TEM images analysis, the histogram of the gold particle size (Figure 5b) can be well-fitted by a Gaussian function with a mean particle diameter of 3.8 nm. The gold cluster distributions in the bulk composite materials were also studied using an X-ray mapping technique. A series of X-ray elemental mapping images (Figure 6) of the as-synthesized samples show that, from a macroscopic view, the gold particles are evenly distributed throughout the composite samples. More densified gold distributions are observed for higher gold content samples. Thus, these morphological studies demonstrated that with use of this novel nonsurfactant templating method, gold nanoparticles have been successfully prepared and dispersed within the mesoporous silica matrix.

The annealed gold−silica nanocomposites retain a distinctive wine-red color, which arises from the surface plasmon resonance (SPR) of gold particles. SPR is characteristic of mesoscale (2−50 nm) particle surfaces because, at this dimension, the electron cloud can oscillate on the particle surfaces and absorb electromagnetic radiation at a particular level of energy.[35] However, smaller nanoparticles (<1−2 nm) do not display this phenomenon because their electrons exist in discrete energy levels, and bulk gold has a continuous absorbance in the UV/vis/IR region. The UV−visible spectra of as-synthesized composite samples show broad plasmon absorbance peaks at around 520 nm with full-width at half-maximum (fwhm) of 160 nm (Figure 7). All the spectra are found to be similar. The peak position and the shape are not significantly affected by the gold concentration. The absorption maxima obtained in this work are comparable with reported spectra of nanosized gold particles dispersed in silica aerogel prepared with other methods.[36,37] Though dominated by the particle size, the exact wavelength and shape of the plasmon absorbance maximum are also known to be affected by particle shape, orientation, and the environment.[38−42] Therefore, the presence of such a well-defined plasmon absorption not only reveals the size scale of gold particles in the nanocomposites but also contributes to

(27) Polarz, S.; Smarsly, B.; Bronstein, L.; Antonietti, M. *Angew. Chem., Int. Ed.* **2001**, *40*, 4417.
(28) Tanev, P. T.; Pinnavaia, T. J. *Science* **1995**, *267*, 865.
(29) Bagshaw, S. A.; Prouzet, E.; Pinnavaia, T. J. *Science* **1995**, *269*, 1242.
(30) Ryoo, R.; Kim, J. M.; Ko, C. H.; Shin, C. H. *J. Phys. Chem.* **1996**, *100*, 17718
(31) Qi, L.; Ma, J.; Cheng, H.; Zhao, Z. *Chem. Mater.* **1998**, *10*, 1623.
(32) Prouzet, E.; Pinnavaia, T. J. *Angew. Chem., Int. Ed. Engl.* **1997**, *36*, 516.
(33) Zhao, D.; Hou, Q.; Feng, J.; Chmelka, B. F.; Stucky, G. D. *J. Am. Chem. Soc.* **1998**, *120*, 6024.
(34) Joo, J.; Hyeon, T.; Hyeon-Lee, J. *Chem. Commun.* **2000**, *16*, 1487.
(35) Shipway, A. N.; Katz, E.; Willner, I. *ChemPhysChem.* **2000**, *1*, 18.
(36) Anderson, M. L.; Rolison, D. R. *Proc. SPIE-Int. Soc. Opt. Eng.* **1999**, *3790*, 38.
(37) Smith, D. D.; Sibille, L. *J. Porous Mater.* **2000**, *7*, 499.
(38) Doremus, R. H.; Rao, P. *J. Mater. Res.* **1996**, *11*, 2834.
(39) Heilweil, E. J.; Hochstrasser, R. M. *J. Chem. Phys.* **1985**, *82*, 4762.
(40) Khlebtsov, N. G.; Bogatyrev, V. A.; Dykman, L. A.; Mellnikov, A. G. *Opt. Spectrosc.* **1996**, *80*, 113.
(41) Kozuka, H. *Proc. SPIE-Int. Soc. Opt. Eng.* **1997**, *3136*, 304.
(42) Bloemer, M. J.; Haus, J. W.; Ashley, P. R. *J. Opt. Soc. Am.* **1990**, *B7*, 790.

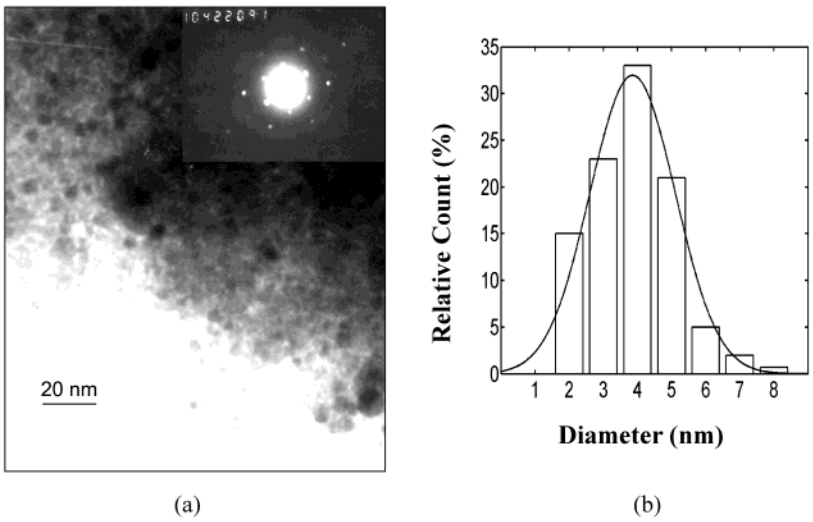

(a) (b)

Figure 5. (a) A representative TEM image of mesoporous gold−silica nanocomposite sample (GS50-10). The darkest round spots are gold nanoparticles. The gray framework feature is a silica matrix with interconnected wormlike pores (lighter feature). Insert: an electron diffraction pattern of gold nanoparticles in the same sample. (b) Size distribution histogram of the gold particles formed and dispersed in the mesoporous silica matrix shown in (a) with a Gaussian curve fitted to the data. About 300 particles were sampled from five different areas in the TEM images. The presence of some gold particles (fewer than 0.3%) with apparent diameters greater than 8 nm might be attributed to aggregation of gold nanoparticles or overlapping images of particles because of the sample thickness.

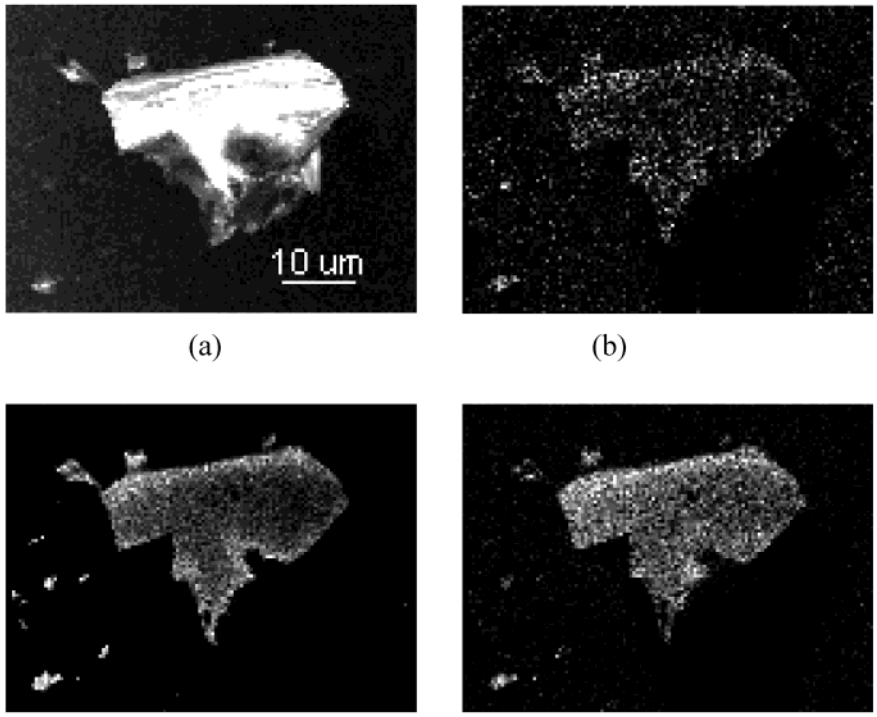

(a) (b)

(c) (d)

Figure 6. Series of X-ray mapping images of mesoporous gold−silica nanocomposite containing 25 wt % gold (GS50-25): (a) As-made nanocomposite; (b) gold mapping; (c) silicon mapping; (d) oxygen mapping.

some other morphological information: the colloidal gold particles in the composites are more likely to be confined in the pore cages, or if co-forming the pore wall with silica, they are more likely to be exposed to the pore surface rather than embedded in the silica matrixes.[37]

Concluding Remarks

In this paper we have presented a facile synthesis of mesoporous gold−silica nanocomposites through a one-step sol−gel reaction. With use of a nonsurfactant compound DBTA as the pore structure directing template, the synthesis process is environment friendly and convenient. The versatility of this method for preparing nanocomposite can be demonstrated with a varied selection of nonsurfactant compound and colloidal nanoparticles. The pore size and pore structure of the nanocomposite are able to be fine-tuned by varying the amount of template or using different template compounds. Here, with DBTA as a nonsurfactant template

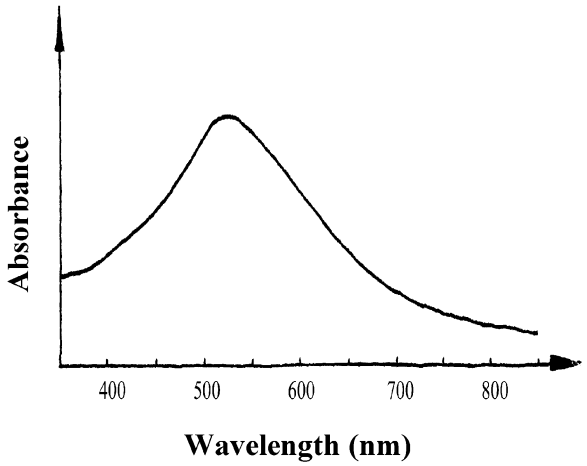

Figure 7. Typical solid-state UV−vis reflectance spectrum of mesoporous gold−silica nanocomposite.

and a gold sol as the source of metal nanoparticles, mesoporous gold−silica nanocomposites have been successfully prepared with this method. Gold particles with the size of 2−8 nm were dispersed throughout the porous silica matrixes. With a gold load as high as up to 10 wt %, the composite materials exhibit mesoporosity with a large surface area, a big pore volume, and relatively narrow pore size distributions. The mesoporous silica matrixes show little effect upon the optical characteristics of gold nanoparticles. Surface plasmon resonance spectra of the gold−silica nanocomposites resemble typical plasmon absorption of gold particles with similar size (i.e., 2−50 nm). Combining both high porosity of the silica framework and the unique physical/chemical properties (such as conductivity and optical behavior) of the second material phase, nanosized gold particles, the mesoporous gold−silica nanocomposite materials are potentially useful for sensors and catalysts. A promising application of using these novel nanocomposites to detect the presence of trace amounts of chemical and biological agents with surface-enhanced Raman spectroscopy is currently under active investigation. The preliminary results show that, with the gold nanoparticles containing silica samples, the limiting detected concentration of cyanide ion in aqueous solution can decrease to 10 ppm. The systematic results of this chemical sensing application study will be reported separately.

Acknowledgment. This project was supported by the US Army Research Office (ARO), the Army Research Laboratory (ARL), and the Commonwealth of Pennsylvania through the Drexel-Penn-Franklin Nanotechnology Institute. We thank Mr. David J. von Rohr of Drexel University for his assistance in energy-dispersive X-ray elemental analysis and obtaining of X-ray mapping images. We are most grateful to three referees for many valuable suggestions, which have materially improved this article.

CM0202106